

Article

Design Studies of Re-Entrant Square Cavities for V-Band Klystrons

M Santosh Kumar ^{1,*}, Santigopal Maity ¹, Soumojit Shee ², Ayan Kumar Bandyopadhyay ³, Debashish Pal ³ and Chaitali Koley ¹

¹ Department of Electronics and Communication Engineering, National Institute of Technology Mizoram, Aizawl 796012, Mizoram, India

² Department of Electronics and Communication Engineering, Institute of Technical Education and Research, Siksha 'O' Anusandhan (Deemed to be University), Bhubaneswar 751030, Odisha, India

³ CSIR-Central Electronics Engineering Research Institute, Pilani 333031, Rajasthan, India

* Correspondence: santosh.ece.phd@nitmz.co.in

Abstract: V-band Klystrons find applications in satellite communications and 5G technology. Here, we present a V-band Klystron using radial re-entrant square cavities (RRSCs). The RRSCs are easy to fabricate, assemble, align, and tune to the operating frequency, which are significant concerns in V-band. We have optimized the number of cavities and the gap for best possible gain and bandwidth. The eigenmode and particle-in-cell (PIC) simulation results of the CST microwave studio are presented. The optimum design uses eleven equidistantly placed RRSCs, producing the maximum gain of 27.17 dB at 60.1 GHz with a bandwidth of ~150 MHz.

Keywords: re-entrant cavity; vacuum electronic amplifiers; V-band Klystron; V-band RF section



check for updates

Citation: Kumar, M.S.; Maity, S.; Shee, S.; Bandyopadhyay, A.K.; Pal, D.; Koley, C. Design Studies of Re-Entrant Square Cavities for V-Band Klystrons. *Electronics* **2023**, *12*, 6. <https://doi.org/10.3390/electronics12010006>

Academic Editor: Massimo Donelli

Received: 19 November 2022

Revised: 8 December 2022

Accepted: 13 December 2022

Published: 20 December 2022



Copyright: © 2022 by the authors. Licensee MDPI, Basel, Switzerland. This article is an open access article distributed under the terms and conditions of the Creative Commons Attribution (CC BY) license (<https://creativecommons.org/licenses/by/4.0/>).

1. Introduction

Klystrons are widely used vacuum electronic amplifiers. They offer high gain and efficiency in a simpler design and a more compact geometry than the Traveling Wave Tubes (TWTs), with narrower bandwidth. Several bandwidth, gain, and power enhancement techniques have been developed over the years of its applications. The bandwidth and gain can be enhanced by stagger tuning of multiple cavities [1–4], extended interaction cavities [5–10], and low-quality factor cavities [11]. Gain can be improved using multiple electron beams [6–8].

The Varian brothers invented the multi-cavity Klystron before World War II as a microwave oscillator and amplifier. The invention eventually evolved into developments of multi-cavity Klystrons, multiple beam Klystrons, extended interaction Klystrons and high-power Klystrons at higher frequencies, including millimeter-wave bands. As the operating frequency increases, the cavity dimension decreases. In the millimeter-wave band, the maximum diameter of the cavity decreases to millimeters, and the diameter of the drift tube through which the electron beam passes decreases to a fraction of mm. Consequently, obtaining a high-power Klystron amplifier with a large gain-bandwidth product has been challenging. The Klystrons overcome the gain limitation by using multiple intermediate cavities in the RF section [6]. To achieve higher gain and bandwidth, a Klystron may employ two types of tuning. Firstly, synchronous tuning—where all Klystron's cavities are tuned to the same frequency [12–14] for gain maximization—and secondly, asynchronous/staggered tuning—where the cavities are kept slightly detuned concerning each other for higher bandwidth. This article reports a V-band Klystron employing synchronous tuning with periodically placed RF cavities.

The RF cavity geometries are optimized to achieve sufficient electric field concentration around the beam. Engineering design of the cavities requires the consideration of several factors such as fabrication tolerances, thermal and other detuning parameters such as

radiation pressure (Lorentz detuning, especially for high power applications) [15], affecting the dimensions of the cavities. The re-entrant types of RF cavities are a very popular choice for Klystrons to achieve all the required cavity parameters such as frequency, Q factor, shunt impedance and R/Q value. Besides the Klystrons, these types of cavities are also used in electromagnetic cavity based transducers, particle accelerators, synchrotron radiation facilities etc. [15,16].

The input RF signal in the first cavity initiates the velocity modulation process. It becomes more pronounced as the beam traverses through the series of intermediate cavities. As a result, the electron beam forms denser bunches, intensifying the induced RF field in the successive intermediate cavities. The electron bunches cross the output cavity's gap while the cavity fields oppose their motion. Under these conditions, maximum energy is transferred from the electron beam to the output cavity. The field grows as the beam's kinetic energy is transferred to the cavity's field.

A novel topology of high frequency Klystrons (operating in higher order mode) has been proposed by Paoloni [17], where simple cavity geometry is employed to overcome high frequency fabrication limitations of conventional re-entrant and extended interaction Klystron cavities. In the current design, the approach of periodically allocated cavities operating in fundamental mode has been followed with the redesign of the RF section for V-band operation. A re-entrant square cavity is designed first as an intermediate cavity of the Klystron [18]. The design is then optimized for the maximum R/Q ratio. A coupler [19] is attached to the cavity to facilitate the input/output, and several intermediate cavities are assembled and aligned to form the Klystron's RF section. PIC simulation is carried out to probe the performance of the proposed Klystron. The optimum number of cavities is also determined to maximize the gain. The designed structure can easily be fabricated with conventional fabrication tools, unlike structurally complicated internal coupling multi-gap cavities [20–22].

Reported Klystrons at this frequency band (around 60 GHz) are rare and, in most of the reported cases of high frequency Klystrons, extended interaction types of topology (with complex geometries) have been utilized. Here, the proposed device is of simple structure, is microfabrication compatible and compact in form factor, offering 256 W of output power.

This paper is organized as follows. Section 2 presents the design equations of the various RRSCs and the RF section, followed by the cold simulation results. Section 3 concentrates on the PIC simulation results and the RF performance of the RRSC Klystron. Finally, Section 4 summarizes the principal findings of the present work and suggested domains for further improvements along with the potential application areas.

2. Design and Operation of RRSC and RF Section

2.1. Design of RRSC

A multi-cavity Klystron amplifier employs two types of cavities—the input/output cavity and the intermediate cavity. The first type facilitates the input of a low-power RF signal and its extraction after amplification. The second type facilitates the production of the required gain. Figure 1 shows a CST model of these two types of RRSCs. Figure 1a shows the input/output cavities. The rectangular i/o coupler allows the RF signal to be fed into the input cavity. It initiates velocity modulation and thereby the bunching of the electron beam. Figure 1b shows one of the intermediate cavities, and Figure 1c shows the cross-section of (b). In a re-entrant cavity, a strong electric field results in the interaction gap 'g' (Figure 1c).

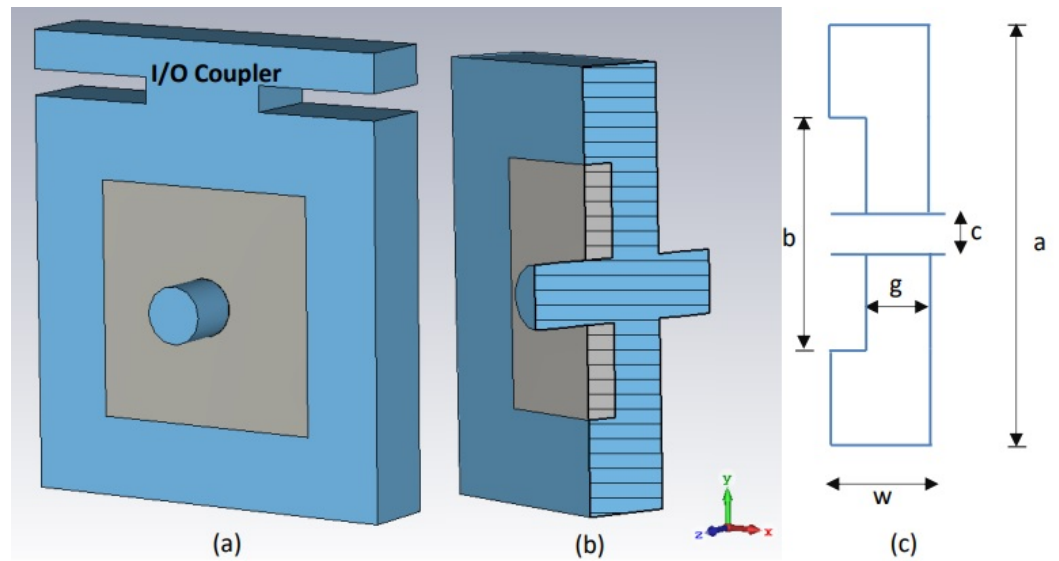


Figure 1. Perspective view of RRSC: (a) input/output cavity, (b) intermediate cavity, and (c) cross section of an intermediate cavity.

The enhanced electric field in the beam passage helps to amplify the RF by way of a more robust velocity modulation. Since the cavities are frequency-selective resonant structures, the operational bandwidth of any Klystron is inherently narrow. However, the bandwidth can be widened by slightly detuning the cavities. This can be done by changing the cavity dimensions, such as the interaction gap ‘g’ or re-entrant height ‘b’ (Figure 1c). However, changing the dimension changes the R/Q value as well. The beam field interaction degrades for a cavity with a low R/Q value. In such cases, it might not establish the required level of beam modulation to achieve the desired gain and output power specifications.

The cavity dimensions and simulation results are listed in Table 1. The Q-factor is defined as 2π times the ratio of the total energy stored to the total energy dissipated per cycle. The ratio R/Q is a figure of merit, dependent only on cavity shape or geometry. The Q-factor and R/Q ratio are calculated in post-processing steps. Here, we have used copper (lossy metal type) ($\sigma = 5.7 \times 10^7$ S/m) as the cavity material and the cavity was considered to be filled with vacuum. The R/Q is calculated as

$$\frac{R}{Q} = \frac{V_g^2}{2\omega W'} \tag{1}$$

where V_g is the interaction gap voltage, ω is the resonant frequency, and W is stored energy. The cavity dimensions are optimized to achieve maximum R/Q ratio without deviating from the design frequency.

Table 1. Dimensions of RRSCs and simulation results.

RRSC Type	Dimension (mm)					Simulation Results		
	a	b	c	w	g	f (GHz)	R/Q (Ω)	Q (Unloaded)
input/output	3	1.8	0.44	0.6	0.395	60	86	1364
intermediate	3	1.7	0.44	0.6	0.38	60	85	1359

a → cavity height; b → re-entrant height; c → beam tunnel radius; w → cavity width; g → beam interaction gap.

2.2. Design of R.F. Section

In order to design the RF section at the proposed frequency of 60 GHz, three fundamental parameters must be determined—(i) the distance between adjacent cavities, (ii) drift tube radius, and (iii) beam radius.

2.2.1. Distance between Adjacent Cavities (d)

It depends on the DC electron velocity v_o . This can be obtained by multiplying the number of electron transit cycles in the drift space (N) with the transmitted beam wavelength (λ_e) given by

$$d = N\lambda_e, \quad (2)$$

where

$$\lambda_e = \frac{2\pi}{\beta_e} = \frac{v_o}{f} = \frac{\sqrt{2\eta V_o}}{f}. \quad (3)$$

Here, f is the operation frequency, β_e is the beam propagation constant, η is the electron charge to mass ratio, and V_o is the beam voltage. Equation (2) can be simplified as

$$d = N \left(\frac{\sqrt{2\eta V_o}}{f} \right), \quad (4)$$

and therefore

$$d = N \left(5.93 \times 10^5 \sqrt{V_o} \right) / f. \quad (5)$$

Here, f is in Hz, V_o is in volts and d is in meters. It is obvious that the distance between adjacent cavities (d) is directly proportional to input electron beam voltage (V_o).

2.2.2. Drift Tube Radius (r)

It is inversely proportional to electron wave number (k),

$$r = \frac{1}{k}, \quad (6)$$

where wave number is the ratio of the angular frequency (ω) and DC velocity of electrons (v_o), i.e.,

$$k = \frac{\omega}{v_o}. \quad (7)$$

2.2.3. Radius of Electron Beam (r_b)

To ensure proper transmission of the electron beam through the drift tube, and to avoid unwanted interception in cavity walls, a typical beam filling factor of 70 % is used. So, the beam radius (r_b) is

$$r_b = 0.7 \times r. \quad (8)$$

2.3. Operation

For proper operation, all cavities constituting the RF interaction region must resonate in the fundamental mode at the design frequency of 60 GHz. The initial dimensions of the cavity shown in Table 1 are calculated using analytical expressions and are subsequently modeled in CST microwave studio as shown in Figure 2. A Klystron amplifier employs a number of intermediate cavities to meet the gain requirement. Higher numbers of intermediate cavities improve the electron bunching. Here, we have used nine intermediate cavities in the Klystron along with one input cavity and one output cavity. The arrangement of the total eleven RRSCs is as shown in Figure 2.

The velocity modulation is significantly increased as the beam gives energy to the RF field in each successive intermediate cavity. The number of cavities and the beam characteristics affect the Klystron's gain. Equation (5) is used to calculate the axial distance between cavities for a particular operating frequency and beam voltage. The inter cavity distance for 60.0 GHz operation with a 20 keV electron beam comes out as 1.4 mm, which is used as the initial value during PIC simulation. The inter-cavity distance is optimized during PIC simulation for maximum power gain and the optimized inter-cavity distance comes out as 1.44 mm. Adding more intermediate cavities in a Klystron is equivalent to adding more stages in a traditional amplifier. Due to the gain bandwidth product limitation,

the overall bandwidth is lowered as the amplifier gain increases. This is known as the synchronous tuning technique in the cascaded amplifier. If the cavities are adjusted to slightly different frequencies, the gain may reduce marginally, but the bandwidth of the device will increase significantly. This tuning technique is known as staggered tuning.

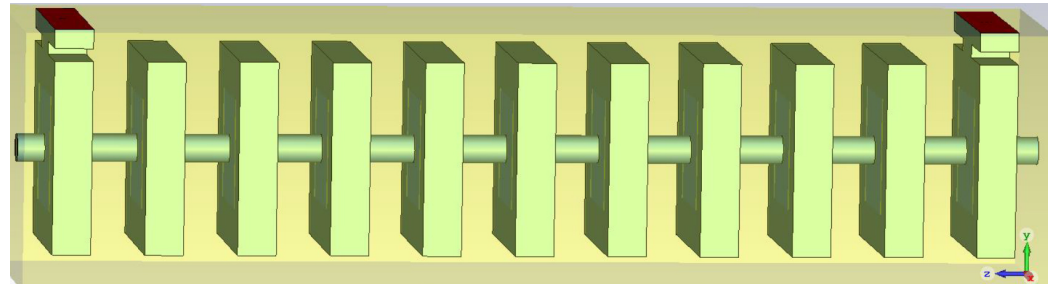


Figure 2. Perspective view of RRSC Klystron in CST microwave studio suite.

3. Simulation Results

After calculating various dimensional parameters of the preliminary design of the RF section, we go for cold simulation using the Eigenmode solver of the CST microwave studio. The advanced Krylov Subspace (AKS) method is used to find the lowest order Eigenmodes for the specified re-entrant boundary condition of our RRSCs. Figure 3a,c show the electric field patterns of the operating mode inside the RRSCs. This mode is favorable for velocity modulation because the electric field maxima occur at the cavity's center, along the beam axis. However, there are fringing fields near the cavity gap but the majority of the field remains parallel to the axis. The corresponding magnetic fields are confined in the orthogonal plane, forming closed loops following the right-hand rule, as shown in Figure 3b,d. The side walls of the cavity are the region of an enormous magnetic field and a small electric field.

In contrast, the gap is a region of tremendous electric and small magnetic fields. Thus, the gap is equivalent to a capacitor, while the cavity walls provide inductance. As the resonant RF field oscillates, the electric energy converts to magnetic energy, and vice versa. The conduction current flows along the inner wall and completes the loop through the displacement current flowing, employing a time-varying electric field through the gap.

In a PIC simulation, an electron beam with its energy corresponding to the applied beam voltage is launched into the R.F. Section. A velocity-modulated electron beam from the input cavity (due to the R.F. signal introduced through the input port) enters the second cavity and subsequent cavities. Because these cavities are unloaded (except for the electron beam) and have higher Q-factors, the beam-induced R.F. field is stored inside the cavities for several resonant cycles, which amplifies the velocity modulation of the beam. The velocity modulation of the beam is gradually increased. The velocity modulation at different time steps (represented by frames) is recorded by phase space monitors in the z-direction (across the beam propagation direction), shown in Figure 4.

After the cold simulation, the performance of the RRSC Klystron is evaluated by the particle in cell (PIC) solver of CST microwave studio [23]. This solver computes the non-linear beam-field interaction in vacuum electronics devices. Copper (Cu) is used as cavity material for high thermal and electrical conductivity. The cylindrical electron beam radius $r_b = 0.15$ mm is determined according to Equation (8), considering 20 KeV energy, and 0.2 A current with beam tunnel radius $r = 0.22$ mm.

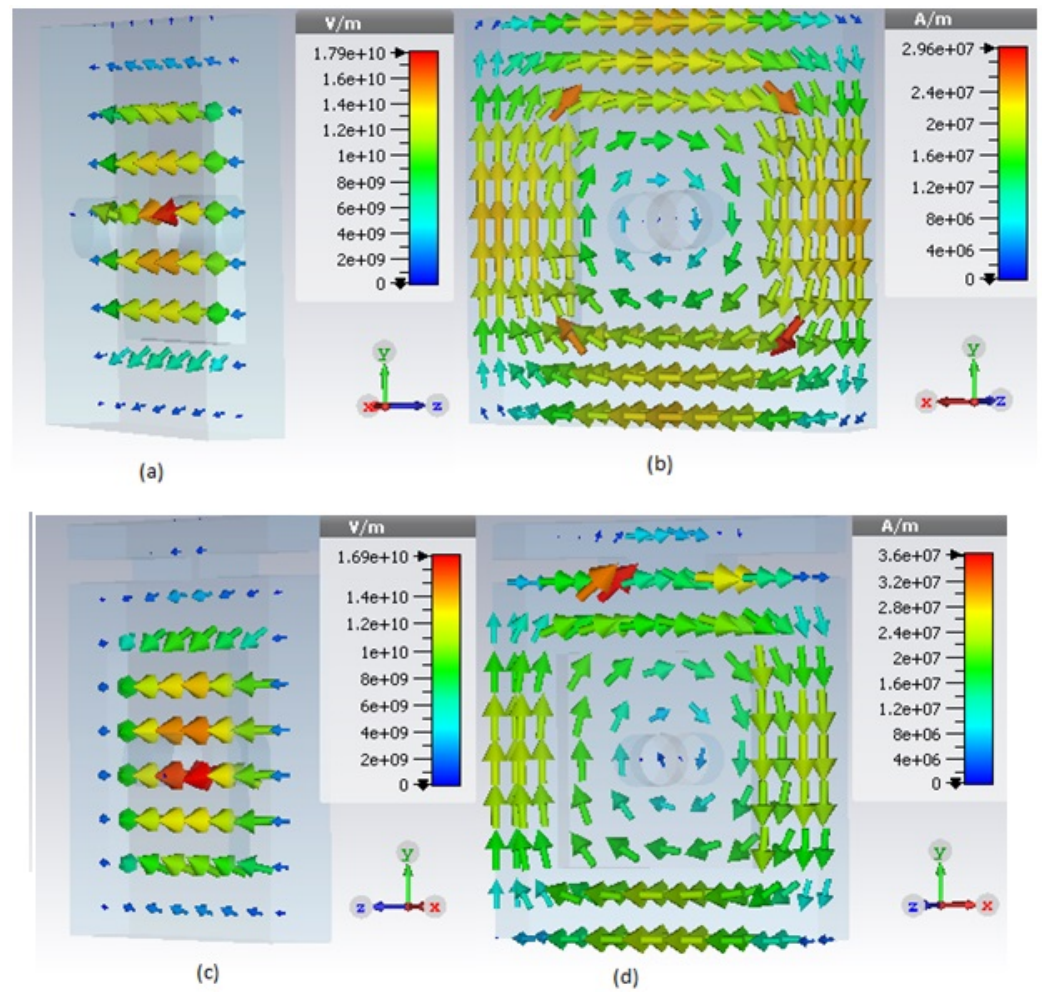


Figure 3. (a) Electric field in intermediate RRSC, (b) Magnetic field in Intermediate RRSC, (c) Electric field in input and output RRSC, and (d) Magnetic field in input and output RRSC.

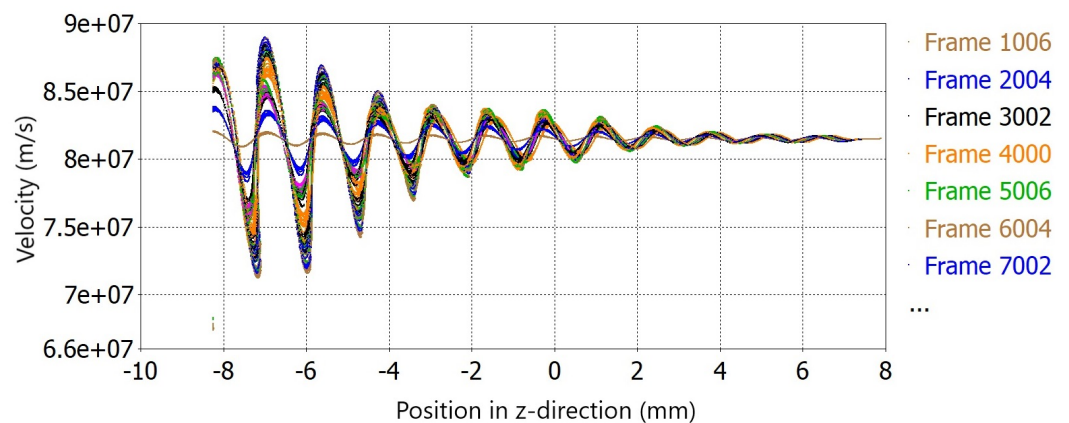


Figure 4. Particle velocity in z-direction.

The device shown in Figure 2 is simulated in a PIC solver for 100 ns with 0.5 W input RF power, and the output from the output cavity is shown in Figure 5. The electrons in a stream of 0.2 A beam current are accelerated by 20 KeV energy in the anode-cathode gap. The accelerated beam faces further acceleration and retardation by the RF field in the cavity gap in each successive intermediate cavity. This interaction of beam kinetic energy with the cavity fields results in velocity modulation. The process continues in the intermediate

cavities, transforming the continuous electron beam into electron bunches. At the output cavity, this bunched beam induces a field of the same frequency as the input RF signal. This induced field grows in amplitude at the expense of the beam’s kinetic energy, which is ensured by the proper placement of the output cavity. The simulation result predicts 256 W peak power at the output cavity, corresponding to a gain of 27.17 dB.

Figure 6 shows how the power gain changes as the number of cavities increases. The RF signal power gain increases proportionally with the rise in cavity numbers. With two cavities, the RRSC Klystron exhibits attenuation of the input signal represented by a negative gain of -5.39 dB; however, with a total of eleven cavities, it exhibits 27.14 dB gain.

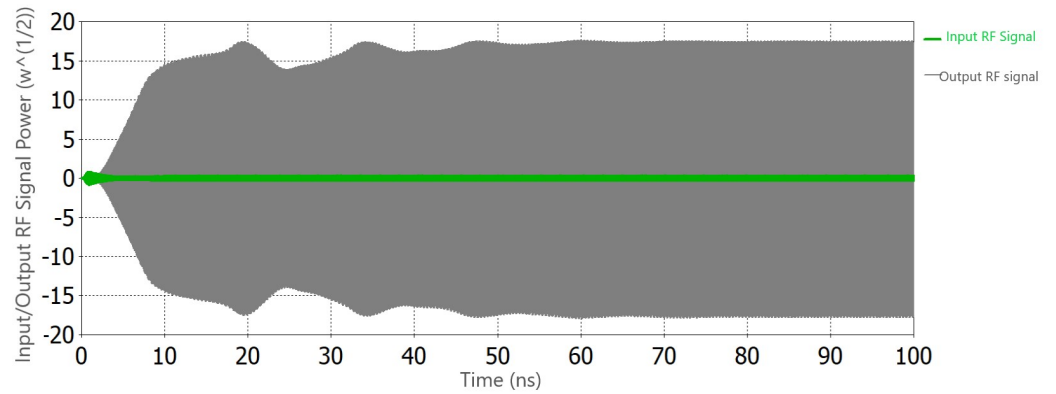


Figure 5. RF input signal and amplified output signal at the input and output cavity ports, respectively.

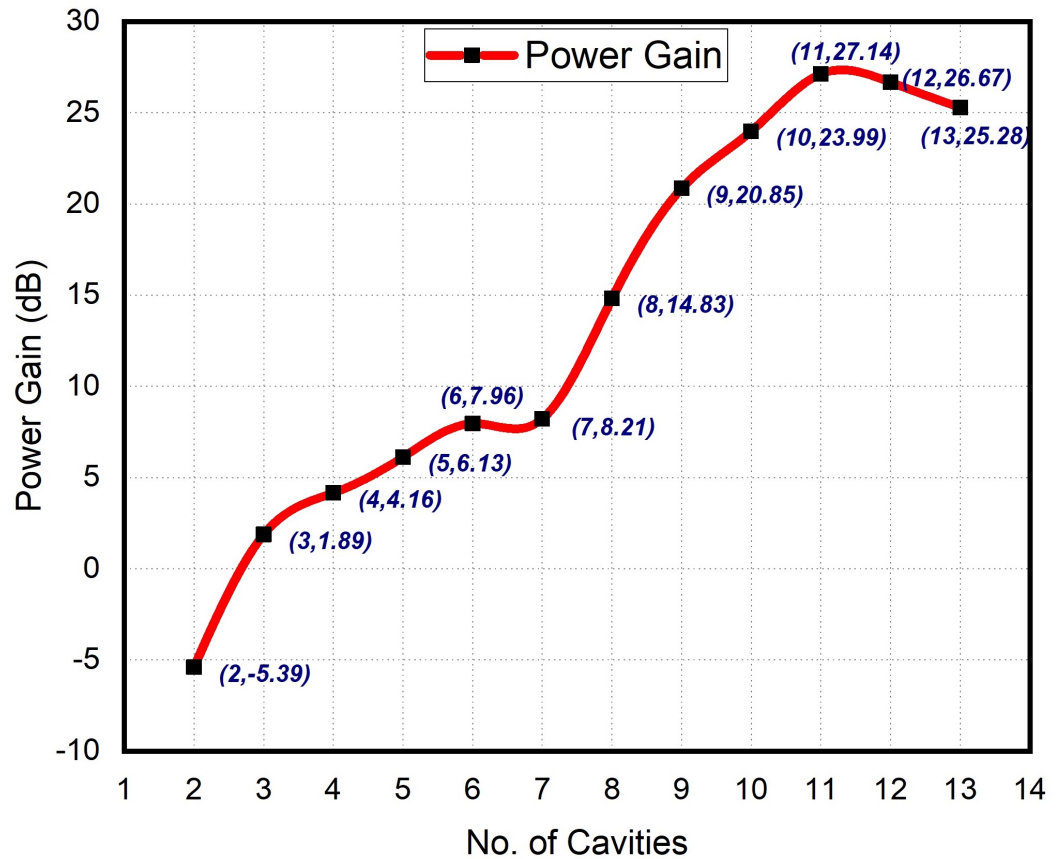


Figure 6. Plot of output power gain vs total number of cavities.

We scanned frequencies ranging from 60 to 60.25 GHz with a step size of 0.025 GHz. The stable output signal power for each frequency point for a specific frequency range

is shown in Figure 7. At 60.1 GHz, the highest output signal power is 256 W, and the saturated gain is 27 dB with a 3 dB bandwidth of more than 150 MHz.

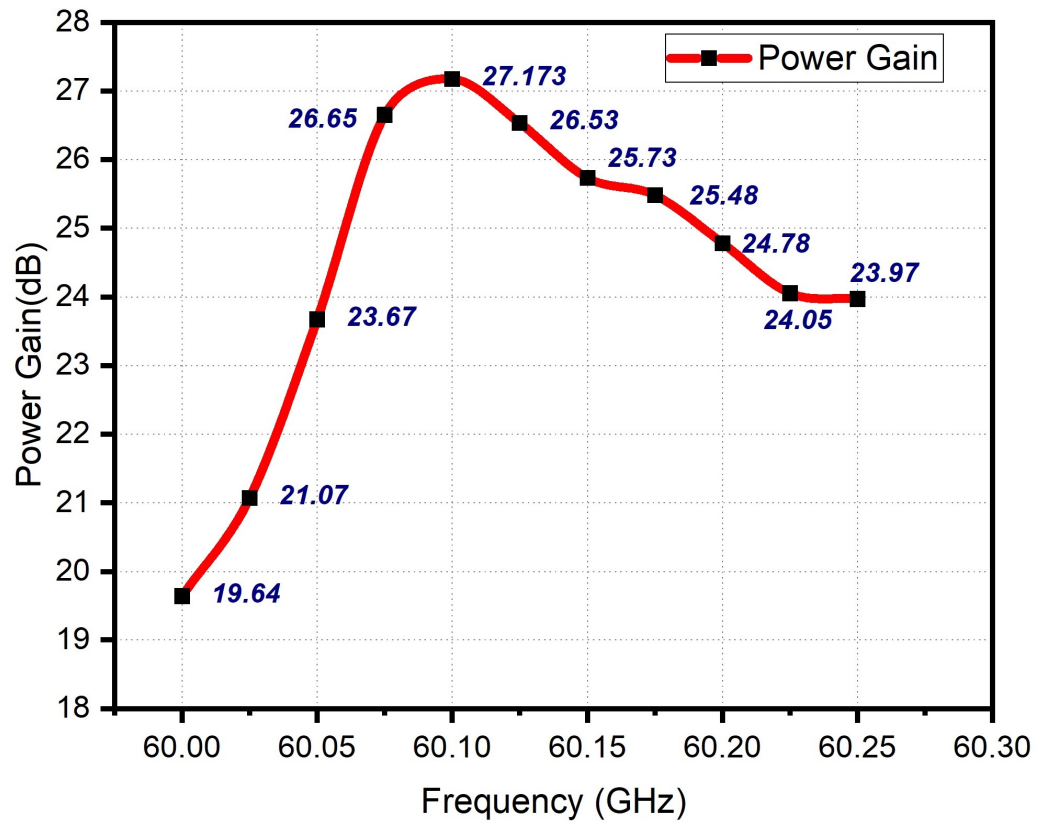


Figure 7. Plot of output power gain vs. input RF signal frequency.

The Fourier transform (FT) of the multi-cavity RRSC Klystron’s output RF signal is shown in Figure 8. The maximum RF output signal is achieved at the central frequency of 60.1 GHz.

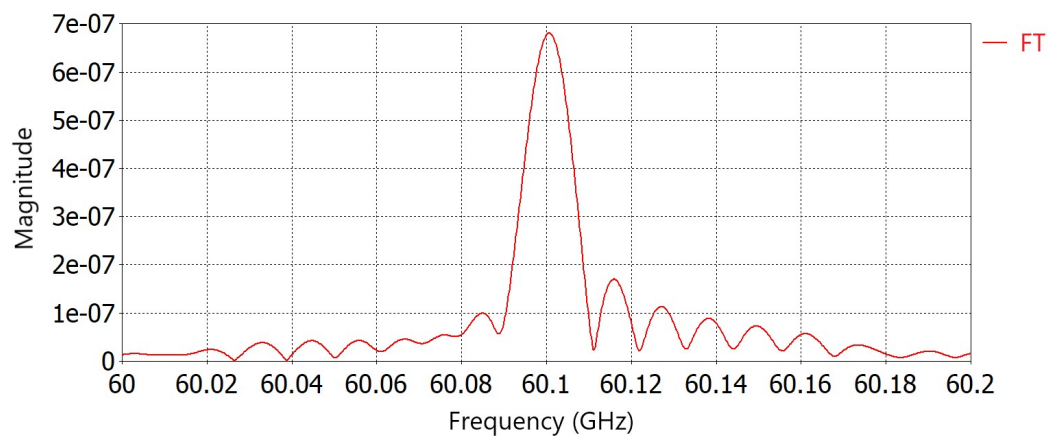


Figure 8. Spectrum of output signal.

4. Conclusions

Here, we have designed a resonant re-entrant square cavity, optimized it for the highest possible interaction impedance, and employed the cavities for the RF section of a V-band Klystron. After that, we optimized the number of cavities for maximum gain. Nine intermediate cavities produced the best result for the synchronous tuned condition of

the device. Simulation results predict a power gain of 27.17 dB over 150 MHz bandwidth, centered at 60.1 GHz frequency.

The proposed RRSC cavities and their assembly forming the RF section are compatible with conventional micro-fabrication and metallic 3D printing technology. The proposed Klystron can be used in subsystems of V-band RADARs, high-speed wireless data communication, and satellite communications.

There is ample scope for improvement in the RF section through extended interaction type cavities to improve the output power and bandwidth, which we are currently exploring.

Author Contributions: Conceptualization, A.K.B., D.P. and C.K.; Methodology, M.S.K., S.M., S.S., A.K.B., D.P. and C.K.; Software, M.S.K. and S.M.; Validation, A.K.B. and D.P.; Formal analysis, M.S.K., S.M. and S.S.; Investigation, A.K.B. and D.P.; Writing—original draft, M.S.K.; Writing—review & editing, S.M., Soumojit Shee, A.K.B., D.P. and C.K.; Supervision, A.K.B. and C.K. All authors have read and agreed to the published version of the manuscript.

Funding: This research was partially funded by IIT Guwahati Technology Innovation and Development Foundation sponsored by Department of Science & Technology (DST) grant number TIH/TD/0303.

Institutional Review Board Statement: Not applicable.

Informed Consent Statement: Not applicable.

Data Availability Statement: Not applicable.

Acknowledgments: The authors would like to thank the IIT Guwahati Technology Innovation and Development Foundation sponsored by Department of Science & Technology (DST) for providing financial assistance to carry out the research work.

Conflicts of Interest: The authors declare no conflict of interest.

References

1. Shin, Y.-M.; Wang, J.-X.; Barnett, L.R.; Luhmann, N.C. Particle-in-cell simulation analysis of a multicavity W-band Sheet Beam Klystron. *IEEE Trans. Electron Devices* **2011**, *58*, 251–258. [\[CrossRef\]](#)
2. Wang, S.; Dong, D.; Pei, S.; Zhou, Z.; Fukuda, S.; Zheng, K. Development of s-band High Power Klystron. *Chin. J. Electron.* **2020**, *29*, 772–778. [\[CrossRef\]](#)
3. Fan, J.; Zhang, Y.; Wang, Y. A 30-kW high-power X-band to ku-band Klystron Frequency multiplier. *IEEE Trans. Electron Devices* **2013**, *60*, 1457–1462. [\[CrossRef\]](#)
4. Zhao, Y.; Li, S.; Huang, H.; Liu, Z.; Wang, Z.; Duan, Z.; Li, X.; Wei, Y.; Gong, Y. Analysis and simulation of a multigap sheet beam extended interaction relativistic Klystron amplifier. *IEEE Trans. Plasma Sci.* **2015**, *43*, 1862–1870. [\[CrossRef\]](#)
5. Chang, Z.; Meng, L.; Yin, Y.; Wang, B.; Li, H.; Rauf, A.; Ullah, S.; Bi, L.; Peng, R. Circuit design of a compact 5-kv W-band Extended Interaction Klystron. *IEEE Trans. Electron Devices* **2018**, *65*, 1179–1184. [\[CrossRef\]](#)
6. Gilmour, A.S. *Klystrons, Traveling Wave Tubes, Magnetrons, Crossed-Field Amplifiers, and Gyrotrons*; Artech House: Norwood, MA, USA, 2011; pp. 281–310.
7. Korolyov, A.N.; Gelvich, E.A.; Zhary, Y.V.; Zakurdayev, A.D.; Poognin, V.I. Multiple-beam Klystron amplifiers: Performance Parameters and Development Trends. *IEEE Trans. Plasma Sci.* **2004**, *32*, 1109–1118. [\[CrossRef\]](#)
8. Gelvich, E.A.; Borisov, L.M.; Zhary, Y.V.; Zakurdayev, A.D.; Pobedonostsev, A.S.; Poognin, V.I. The new generation of high-power multiple-beam Klystrons. *IEEE Trans. Microw. Theory Tech.* **1993**, *41*, 15–19. [\[CrossRef\]](#)
9. Symons, R.S. High Performance Extended Interaction Output Circuit. U.S. Patent 4931695, 5 June 1990.
10. Lin, F.-M.; Li, X.-P. Monotron oscillation in double-gap coupling output cavities of multiple-beam Klystrons. *IEEE Trans. Electron Devices* **2014**, *61*, 1186–1192. [\[CrossRef\]](#)
11. Slater, J.C. *Microwave Electronics*; Dover: New York, NY, USA, 1969; pp. 232–237.
12. Liao, S.Y. *Microwave Devices and Circuits*, 3rd ed.; Prentice Hall: Englewood Cliffs, NJ, USA, 1985; pp. 242–272.
13. Naidu, V.B.; Datta, S.K.; Kumar, L. Two cavity W-band sheet beam extended interaction Klystron simulation. In Proceedings of the 2013 IEEE 14th International Vacuum Electronics Conference (IVEC), Paris, France, 21–23 May 2013. [\[CrossRef\]](#)
14. Nguyen, K.T.; Pasour, J.; Wright, E.L.; Pershing, D.E.; Levush, B. Design of a G-band sheet-beam extended-interaction Klystron. In Proceedings of the 2009 IEEE International Vacuum Electronics Conference, Rome, Italy, 28–30 April 2009. [\[CrossRef\]](#)
15. Kneisel, P. State of the Art of Multicell SC Cavities and Perspectives. In Proceedings of the 8th European Particle Accelerator Conference, Vienna, Austria, 26–30 June 2000; European Physical Society, Inter-divisional Group on Accelerators: Geneva, Switzerland, 2000; pp. 139–143.

16. Blair, D.G.; Ivanov, E.N.; Tobar, M.E.; Turner, P.J.; van Kann, F.; Heng, I.S. High sensitivity gravitational wave antenna with parametric transducer readout. *Phys. Rev. Lett.* **1995**, *74*, 1908. [[CrossRef](#)] [[PubMed](#)]
17. Paoloni, C. Periodically allocated reentrant cavity Klystron. *IEEE Trans. Electron Devices* **2014**, *61*, 1687–1691. [[CrossRef](#)]
18. Kumar, M.S.; Koley, C.; Pal, D.; Maity, S.; Bandyopadhyay, A.K. Design of the radio frequency section of a V-band Klystron. In Proceedings of the 2021 22nd International Vacuum Electronics Conference (IVEC), Rotterdam, The Netherlands, 27–30 April 2021. [[CrossRef](#)]
19. Paoloni, C.; Mineo, M.; Yin, H.; Zhang, L.; He, W.; Robertson, C.W.; Ronald, K.; Phelps, A.D.R.; Cross, A.W. Microwave Coupler for w-band micro re-entrant square cavities. *IET Microwaves Antennas Propag.* **2016**, *10*, 764–769. [[CrossRef](#)]
20. Xie, B.; Zhang, R.; Wang, Y.; Wang, H.; Zhang, X.; Chao, Q.; Liu, K.; Geng, Z.; Liao, Y.; Yang, X. Design of a high-power V-band Klystron with internal coupling Multigap cavity. *IEEE Trans. Electron Devices* **2022**, *69*, 2644–2649. [[CrossRef](#)]
21. Xie, B.; Zhang, R.; Wang, Y.; Zhang, X.; Chen, H. Design of a high-power V-band Klystron based on novel coupling cavity with ridges loading in the middle. In Proceedings of the 2021 Photonics & Electromagnetics Research Symposium (PIERS), Hangzhou, China, 21–25 November 2021. [[CrossRef](#)]
22. Wessel-Berg, T. *A General Theory of Klystrons with Arbitrary, Extended Interaction Fields*; Microwave Laboratory: Stanford, CA, USA, 1957.
23. CST 2018. User's Manual. CSST. Available online: www.cst.com (accessed on 20 August 2020).

Disclaimer/Publisher's Note: The statements, opinions and data contained in all publications are solely those of the individual author(s) and contributor(s) and not of MDPI and/or the editor(s). MDPI and/or the editor(s) disclaim responsibility for any injury to people or property resulting from any ideas, methods, instructions or products referred to in the content.